Equilibrium shoreline response of a high wave energy beach

M. L. Yates,[1,2] R. T. Guza,[1] W. C. O'Reilly,[1] J. E. Hansen,[3,4] and P. L. Barnard[3]

Received 25 September 2010; revised 6 January 2011; accepted 20 January 2011; published 15 April 2011.

[1] Four years of beach elevation surveys at Ocean Beach, San Francisco, California, are used to extend an existing equilibrium shoreline change model, previously calibrated with fine sand and moderate energy waves, to medium sand and higher-energy waves. The shoreline, characterized as the cross-shore location of the mean high water contour, varied seasonally by between 30 and 60 m, depending on the alongshore location. The equilibrium shoreline change model relates the rate of horizontal shoreline displacement to the hourly wave energy E and the wave energy disequilibrium, the difference between E and the equilibrium wave energy that would cause no change in the present shoreline location. Values for the model shoreline response coefficients are tuned to fit the observations in 500 m alongshore segments and averaged over segments where the model has good skill and the estimated effects of neglected alongshore sediment transport are relatively small. Using these representative response coefficients for 0.3 mm sand from Ocean Beach and driving the model with much lower-energy winter waves observed at San Onofre Beach (also 0.3 mm sand) in southern California, qualitatively reproduces the small seasonal shoreline fluctuations at San Onofre. This consistency suggests that the shoreline model response coefficients depend on grain size and may be constant, and thus transportable, between sites with similar grain size and different wave climates. The calibrated model response coefficients predict that for equal fluctuations in wave energy, changes in shoreline location on a medium-grained (0.3 mm) beach are much smaller than on a previously studied fine-grained (0.2 mm) beach.

Citation: Yates, M. L., R. T. Guza, W. C. O'Reilly, J. E. Hansen, and P. L. Barnard (2011), Equilibrium shoreline response of a high wave energy beach, *J. Geophys. Res.*, *116*, C04014, doi:10.1029/2010JC006681.

1. Introduction

[2] Erosion threatens coastal infrastructure and tourism revenues, creating a need for numerically efficient beach change models that parameterize shoreline retreat during storms and recovery during wave energy lulls. Bulk beach response models are by design numerically fast, and use heuristic, observation-based rules, rather than detailed models of fluid and sediment dynamics, to relate changes in beach morphology to changing waves. Existing bulk response models include average wave correlation models [e.g., *Aubrey et al.*, 1980; *Miller and Dean*, 2007; *Quartel et al.*, 2008] and equilibrium beach change models [e.g., *Dean*, 1977, 1991; *Larson and Kraus*, 1989; *Dubois*, 1990; *Davidson et al.*, 2010]. The observations of beach response to a wide range of wave conditions needed to fully validate and calibrate these essentially phenomenological models are lacking, and model development instead relies on the limited available observations of storm, seasonal, and interannual variations in wave energy and beach morphology. Accurate characterization of shoreline location changes at these timescales is a first step toward realistic simulations of beach response over longer timescales.

[3] Correlation models relate the present beach state to recent (e.g., averaged over days to months, and sometimes time-lagged) wave properties. Beach 'state' variables include shoreline location [*List and Farris*, 1999; *List et al.*, 2006; *Davidson and Turner*, 2009], beach volume [*Haxel and Holman*, 2004; *Quartel et al.*, 2008], and the temporal component of EOF modes representing shoreline or profile change [*Aubrey et al.*, 1980; *Larson et al.*, 2000; *Miller and Dean*, 2006]. Averaged wave parameters include, for example, the breaking wave height H_b, the wave energy E, or the nondimensional fall velocity $\Omega = H_b/(w_s T)$, also known as Dean's parameter, where w_s is the fall velocity and T is the wave period [*Miller and Dean*, 2007]. *Wright et al.* [1985] and many others have demonstrated the importance of including the recent (weeks to months) history of the wavefield in correlation models. Beach state and wave conditions are correlated poorly at short (hours to days) timescales because wave conditions often vary much faster than the beach morphology adjusts (e.g., during storm spin-up and spin-down [*Morton*

[1]Scripps Institution of Oceanography, University of California, San Diego, La Jolla, California, USA.
[2]Now at Bureau de Recherches Géologiques et Minières, Orléans, France.
[3]Pacific Science Center, United States Geological Survey, Santa Cruz, California, USA.
[4]Department of Earth and Planetary Science, University of California, Santa Cruz, California, USA.

0148-0227/11/2010JC006681

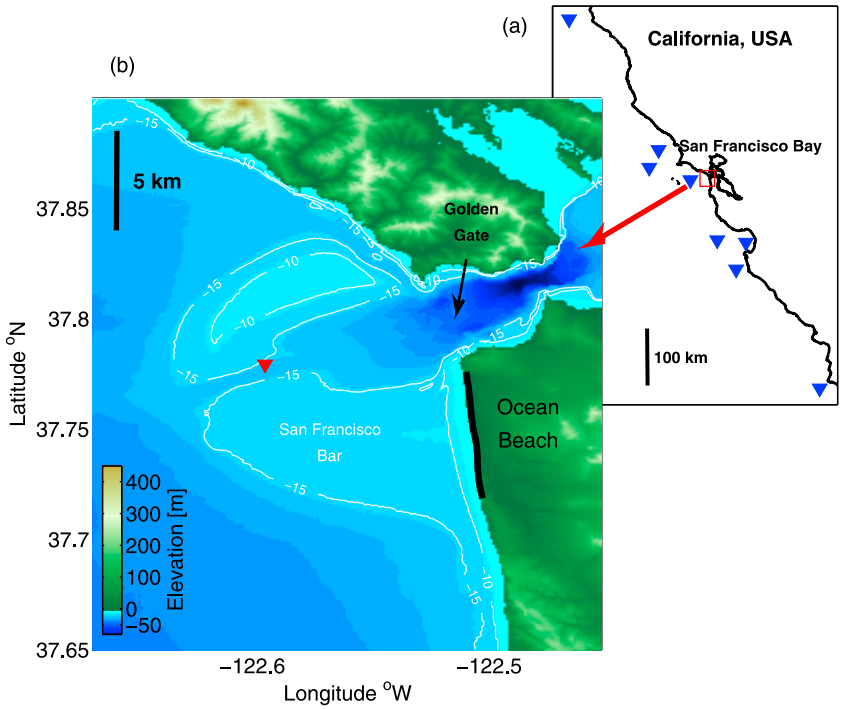

Figure 1. (a) Map of northern California showing locations (blue triangles) of directional wave buoys used to estimate conditions at the Ocean Beach study site (red box). (b) Location of Ocean Beach (thick black line), nearshore wave buoy observation and model comparison (red triangle), Golden Gate, and the San Francisco Bar.

et al., 1995; *Lee et al.*, 1998]). A shortcoming of averaging recent wave conditions is that the timing of events within the averaging interval is neglected. *Quartel et al.* [2008] compared seasonal and storm response observations of beach width and volume change with 8 day and monthly averages of wave parameters, and suggested the sometimes low correlations resulted from neglecting the timing of wave events within the averaging periods.

[4] Equilibrium models relate the rate of beach state change (rather than beach state) to rapidly varying (e.g., hourly or daily) wave properties. Equilibrium models can resolve individual storms and account for the storm sequencing, and are also numerically fast. *Bruun* [1954] first developed the concept of an equilibrium beach profile using hundreds of observed beach profiles. Subsequent equilibrium beach change models rely on the hypothesis that a beach exposed to steady wave conditions evolves toward a unique, wave condition dependent, equilibrium beach profile, with no further change after equilibrium is reached [*Dean*, 1991]. *Wright et al.* [1985] suggested that the rate of beach change toward equilibrium depends on the current wave conditions and the disequilibrium of the wave conditions with the present beach configuration.

[5] Following *Wright et al.* [1985] and *Miller and Dean* [2004], *Yates et al.* [2009] developed a shoreline change model using observations from Torrey Pines Beach, California and two nearby sites, all with similar grain size (0.2 mm median diameter, fine-grained sand on the Udden-Wentworth scale [*Wentworth*, 1922]) and wave climates (moderate energy winter storm waves, with significant wave heights usually ranging between 2 and 4 m, and prolonged summer lulls with significant wave heights less than 1 m). Using tuned parameters, with similar optimal values at the three sites, modeled and observed shoreline locations were well correlated. At San Onofre State Beach, a fourth site with similar waves and coarser sand (0.3 mm diameter, medium-grained sand on the Udden-Wentworth scale), shoreline displacements were small, about 3 m, compared with 30 m at the sites with finer sand. The small shoreline displacements at San Onofre were alongshore variable, possibly not dominated by cross-shore sediment transport processes, and were not used for quantitative model calibration.

[6] Here, the *Yates et al.* [2009] equilibrium model for shoreline location is extended to a medium sand grain (0.3 mm) beach using observations from Ocean Beach, San Francisco, California, a high-energy beach described in section 2. The model is briefly reviewed, and Ocean Beach free parameter values are estimated in section 3. The variability of model free parameter values between sites, alternative model formulations, differences between this model and *Davidson et al.* [2010], and results of a correlation model, are discussed in section 4. Section 5 is a summary.

2. Observations

[7] The study site, a 7 km long, west facing reach at Ocean Beach, San Francisco, California, USA, is located immediately south of the Golden Gate tidal inlet that flushes San Francisco Bay (Figure 1). Mean and maximum spring tidal ranges are 1.25 and 2.65 m, respectively [*National Oceanic and Atmospheric Administration*, 2010]. Ocean Beach is adjacent to the bay mouth, and tidal currents are strong (up

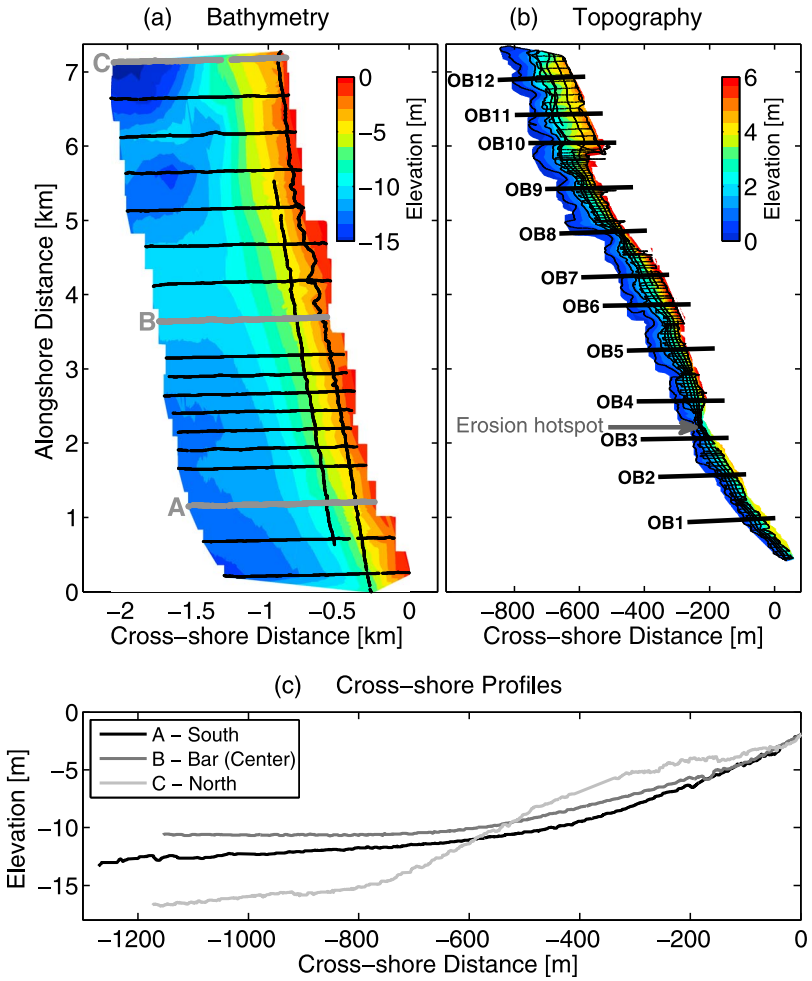

Figure 2. (a) November 2006 bathymetry survey spanning from about 15 m depth to the backbeach (i.e., dunes, revetment), with black lines showing the densely spaced data points. (b) April 2004 beach face survey covering the subaerial beach from the waterline to the backbeach, with thin black lines indicating the closely spaced data points. The thick black lines indicate the centers of the 500 m long alongshore sections (OB1–OB12) in which the observations were averaged. (c) Depth versus cross-shore location on transects A, B, and C, with the transect locations indicated in Figure 2a.

to 1 m/s [*Barnard et al.*, 2007]), particularly at the northern end of the site, closest to the inlet.

[8] The complex nearshore bathymetry includes the San Francisco Bar, an ebb tidal delta west of the bay mouth (outlined by the 15 m depth contour, Figure 1b), which attaches to the shoreline at alongshore coordinate 4 km (Figure 2a). The backbeach barrier varies alongshore, consisting of seawalls, bluffs (often armored with rip-rap), and vegetated dunes.

2.1. Sand Level Surveys

[9] Seasonally averaged shoreline beach slopes (defined between mean sea level (MSL) and mean high water (MHW)) range from 0.03 to 0.06, and the alongshore uniform median sand grain size is approximately 0.3 mm (see *Barnard et al.* [2007] and *Hansen and Barnard* [2010] for details). Seasonally averaged beach width, calculated as the distance from the backbeach barrier to the MHW contour, ranges from less than 20 m in the southern end (near the erosion hot spot (Figure 2b)), to approximately 130 m at the northern end. Fifty-nine sand level surveys were collected between April 2004 and January 2009 with a GPS-equipped all-terrain vehicle (ATV) at low tide. Surveys were separated between 2 days and 4 months, with most surveys approximately 1 month apart.

[10] Time series of horizontal displacements of mean sea level (MSL = 0.975 m), mean high water (MHW = 1.619 m), and mean higher high water (MHHW = 1.805 m) contours are mutually correlated ($R^2 > 0.7$). MHW contour location changes are about 20% less than MSL changes (averaged across all alongshore sections). The MSL contour was underwater (and therefore inaccessible) during some shoreface surveys, so the MHW contour was used as a proxy for the shoreline location, following *Hansen and Barnard* [2010]. The shoreline location was defined on cross-shore transects spaced every 100 m alongshore. The temporal mean was removed from each of the twelve 500 m alongshore sections

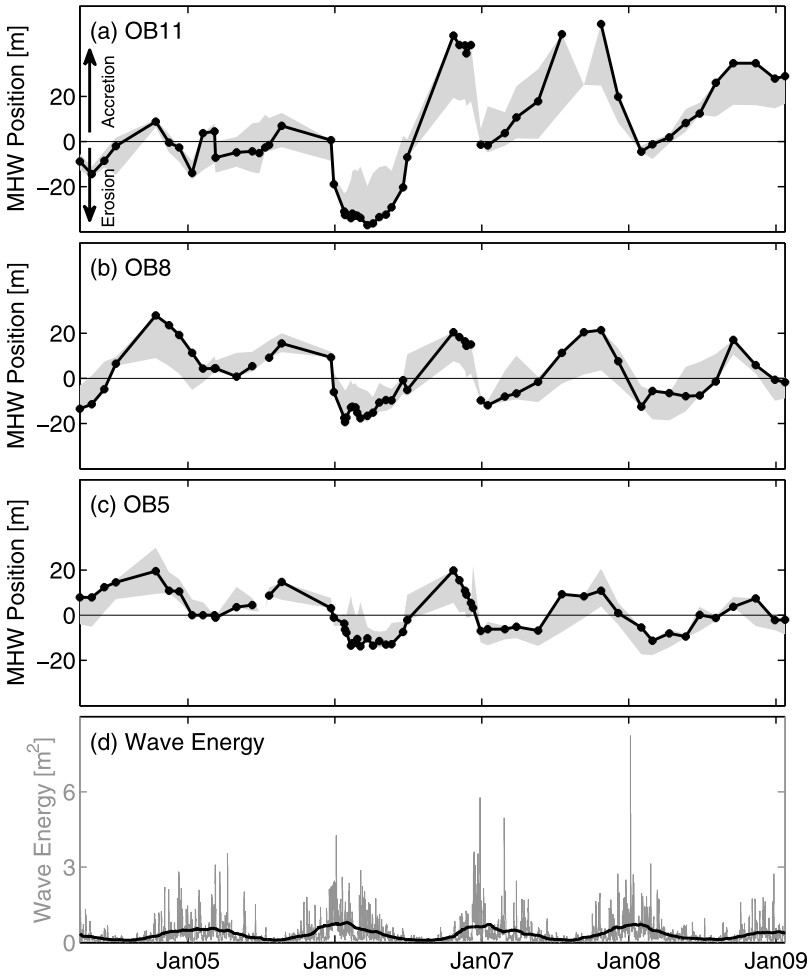

Figure 3. Shoreline position (cross-shore location of the MHW contour with the temporal mean removed) versus time at Ocean Beach alongshore sections (a) OB10–OB12, (b) OB7–OB9, and (c) OB4–OB6. The black line shows the center transect (OB11 (Figure 3a), OB8 (Figure 3b), and OB5 (Figure 3c)) in each group, and the gray shading indicates the range of contour locations on adjacent transects. (d) Hourly wave energy (thin gray line) E and 90 day average $\overline{E}$ (thick black line) at OB5 versus time.

(Figure 2b), and shoreline changes were averaged within each section to reduce the effects of small-scale features.

[11] Shoreline (MHW) locations have a strong seasonal signal in all 500 m sections. The beach is widest in summer and narrowest in winter, and the magnitude of the seasonal cycles varies alongshore between about 30 m and 60 m (Figures 3a–3c). The southernmost region was often inaccessible owing to an erosion "hot spot" (Figure 2b) [*Hansen and Barnard*, 2010], and due to the large data gaps, shoreline changes in sections OB1–OB3 are not considered further. Alongshore sections OB4, OB6, and OB7 have a common multiyear erosional trend (Appendix A), and alongshore sections OB10–OB12 accreted significantly during the summer of 2006 (Figure 3a). These anomalous changes are not associated with corresponding fluctuations in wave energy, and are therefore not captured by the equilibrium model (section 3.2). The remaining sections (OB5, OB8, and OB9) do not have long-term trends during the survey period. *Hansen and Barnard* [2010] suggest that the shift from shoreline locations showing multiyear erosion to accretion is caused by a long-term rotational trend of the shoreline and the effects of the attachment of the San Francisco Bar to the shoreline near alongshore distance 4 km in Figure 2a.

2.2. Waves

[12] Wave blocking by the Farallon Islands (40 km West of Ocean Beach), and wave refraction and focusing by the San Francisco Bar (Figure 1b), create alongshore variations in Ocean Beach waves [*Eshleman et al.*, 2007]. Offshore wave observations (location shown in Figure 1a, blue triangles) are transformed using a spectral refraction wave model [*O'Reilly and Guza*, 1998]. Swell (0.04–0.1 Hz) and sea waves (0.08–0.5 Hz) are initialized with buoys within a radius of 400 and 125 km, respectively, of the prediction location. (Stations 46213, 46214, 46218, 46236, and 46239 are maintained by the Coastal Data Information Program (CDIP), and stations 46013, 46026, and 46042 are maintained by the National Data Buoy Center (NDBC).) Modeled significant wave heights agree well with observations at the CDIP San Francisco Bar buoy (BP142, Figure 4, location

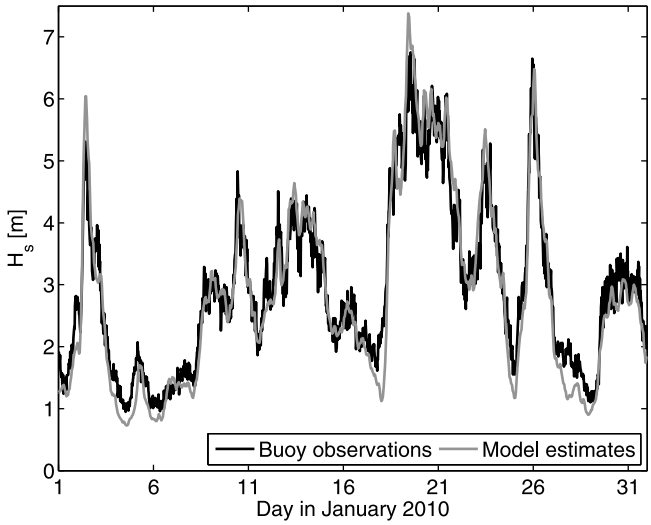

Figure 4. Hourly modeled and 30 min observations of significant wave height at the CDIP San Francisco Bar buoy (BP142), located on the north edge of the entrance channel (red triangle, Figure 1b).

shown in Figure 1b). Spectral wave properties are estimated hourly along the 10 m depth contour every 200 m alongshore, and the wave energy (normalized by ρg^2) estimates are averaged over the same 500 m sections as the shoreline observations.

[13] The seasonal cycle in wave energy is strong, with energetic winter storm waves and lower-energy summer waves (Figure 3d). Wave energy time series are in phase at each alongshore section, but the magnitude of wave events varies alongshore. Wave energy is highest near the center of the surveyed reach, with values up to 3 times larger than the northern (OB12) and southern (OB1) sections during storm events (Figure 5).

3. Equilibrium Model

3.1. Model Formulation

[14] The equilibrium shoreline change model was developed with more than 5 years of surveys at Torrey Pines Beach, California [*Yates et al.*, 2009]. The horizontal shoreline change rate is assumed proportional to the square root of the hourly averaged wave energy $E^{1/2}$ and wave energy disequilibrium ΔE

$$\frac{dS}{dt} = C^{\pm} E^{1/2} \Delta E, \tag{1}$$

where S is the shoreline location, $C^{\pm}$ are change rate coefficients, and ΔE is the energy disequilibrium, given by

$$\Delta E(S) = E - E_{eq}(S). \tag{2}$$

[15] For simplicity, the equilibrium wave energy (the E that causes no change to the present shoreline position S) is assumed to depend linearly on S

$$E_{eq}(S) = aS + b, \tag{3}$$

where a and b are the slope and y intercept, respectively. The sign of the shoreline change rate dS/dt (1) is determined by the sign of the energy disequilibrium ΔE (2). The change magnitude is proportional to ΔE, multiplied by the factor $E^{1/2}$, which reduces dS/dt when E is small (with the limit that $dS/dt = 0$ when $E = 0$), and increases dS/dt when E is large and increased sediment transport is anticipated.

[16] The model assumption that shoreline contour displacement depends on wave energy, and not on wave direction or alongshore gradients in waves and currents, implies that cross-shore sediment flux gradients control shoreline change. Optimal values for the four model free parameters ($C^{\pm}$, a, and b) are determined by minimizing the root-mean-square (RMS) misfit to observations [*Yates et al.*, 2009], and alternative model formulations, including a reduction in the number of model free parameters, are discussed in section 4.2.

[17] In (3), for a given shoreline position S, the equilibrium wave energy E_{eq} causes no further change. Conversely, for a given wave energy E, rearranging (3) yields the equilibrium shoreline position

$$S_{eq}(E) = \frac{E - b}{a}. \tag{4}$$

When the wave energy E time series is a step function, either increasing or decreasing to fixed level and remaining constant

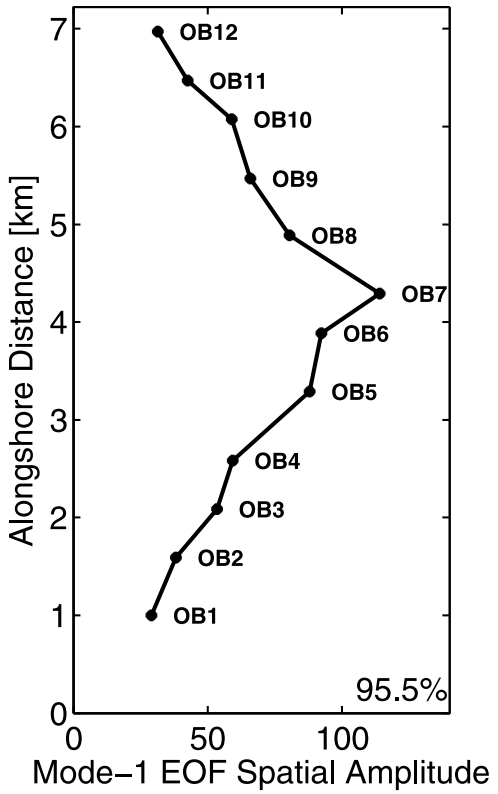

Figure 5. Alongshore variability of the mode 1 EOF spatial amplitude of wave energy at Ocean Beach, representing 95.5% of the variance of the time series at the 12 alongshore sections. The mode 1 EOF temporal amplitude (not shown) is similar to the hourly wave energy time series (Figure 3d).

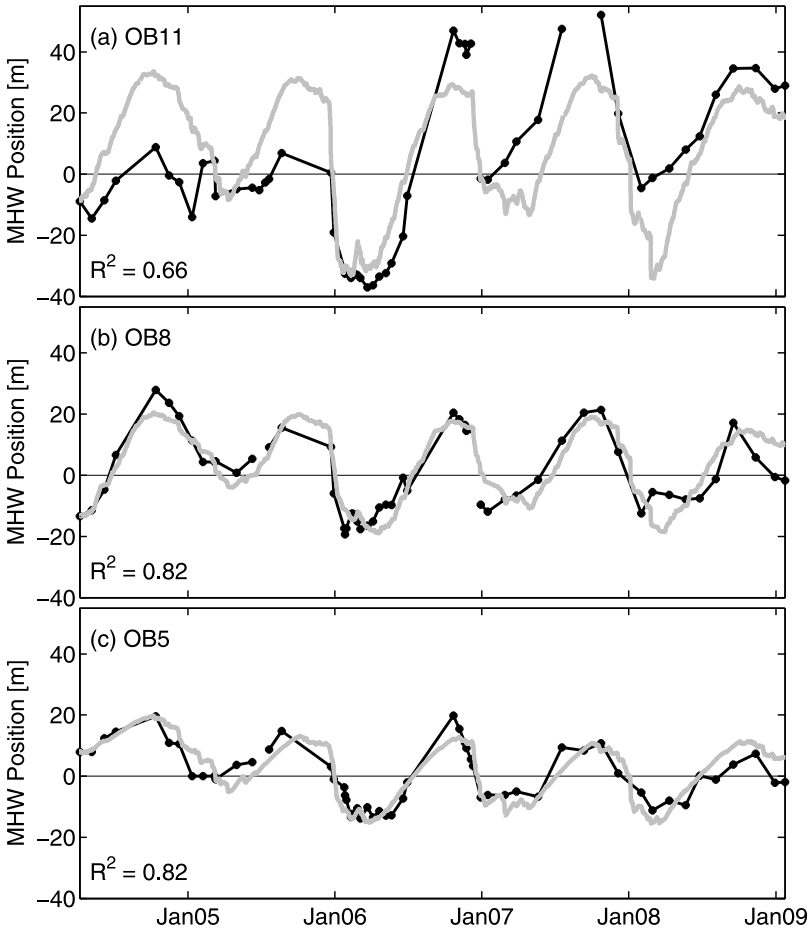

Figure 6. Weekly to monthly observations of MHW contour position with the temporal mean removed (black) and hourly model results (gray) versus time at Ocean Beach sections (a) OB11, (b) OB8, and (c) OB5.

thereafter, the shoreline approaches equilibrium exponentially (consistent with previous models [e.g., *Larson and Kraus*, 1989; *Miller and Dean*, 2004])

$$S(t) = \left(S_0 - S_{eq}\right)e^{-aC^{\pm}E^{1/2}t} + S_{eq}, \tag{5}$$

where S_0 is the initial shoreline position, and S_{eq} is the equilibrium shoreline position for the wave energy E. With equal aC^{+} and aC^{-}, the e-folding scale $[aC^{\pm}E^{1/2}]^{-1}$ is shorter (e.g., the response is faster) with higher-energy waves.

[18] The e-folding scale and thus the rate at which the beach approaches equilibrium is independent of the free parameter b. However, b determines the relationship between the shoreline location S and the equilibrium wave energy E_{eq}, and depends on the magnitude of S, which is defined here as fluctuations about the temporal mean shoreline location.

3.2. Model Fit

[19] Using model free parameters optimized independently for each 500 m alongshore section, the model reproduces the observed seasonal cycle at Ocean Beach and part of the multiyear erosional trend observed at sites OB4–OB7. The squared correlation R^2 between modeled and observed shoreline location varies between about 0.4 and 0.8 (Figure 6). Some R^2 are lower than observed at any southern California site (Figure 7, see *Yates et al.* [2009] for more details). The most unreliable estimates of free parameters, at locations where $R^2 < 0.60$ (OB4, OB6, OB7, and OB12; grey squares at Ocean Beach in Figure 7) are not included in the site average parameter values. At locations OB6, OB7, and OB12, it is suspected that the R^2 correlations are relatively low because of multiyear trends possibly associated with neglected variations in alongshore sediment transport (Appendix A and Figure 8). The causes of low R^2 at OB4 are unknown. In the retained sections, model RMS errors are largest in the northern sections, where the large accretion event in summer 2006 is not reproduced by the equilibrium model (Figure 6a).

4. Discussion

4.1. Model Free Parameters

[20] Model best-fit free parameters in the retained Ocean Beach locations vary alongshore, similar to the southern California sites (Figure 7). The ranges of free parameters for which the model-observations RMS increases by less than 10% (horizontal lines in Figure 7), show the relative insensitivity of the model error to changes in model free

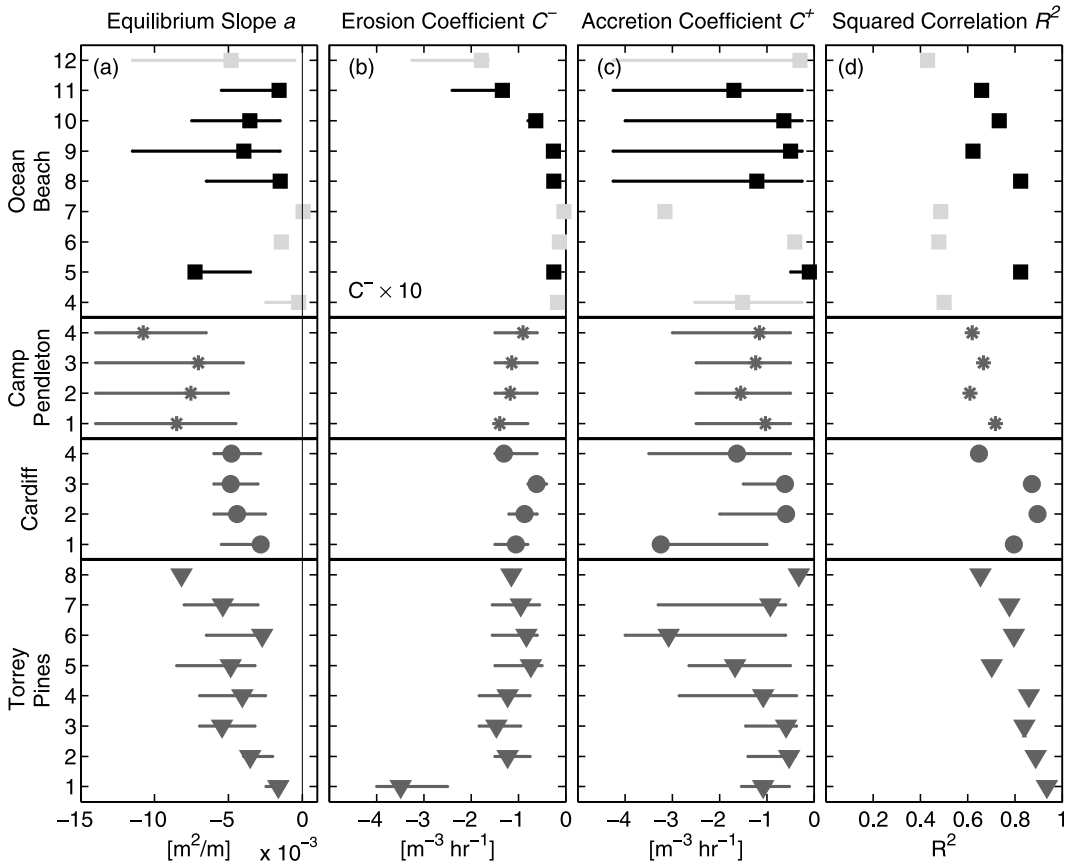

Figure 7. (a–c) Values of best-fit model free parameters at 500 m spaced, numbered alongshore locations (see Figure 2b) at Ocean Beach (squares), and previously tested southern California beaches (Camp Pendleton (asterisks), Cardiff (circles), and Torrey Pines (triangles)). The horizontal lines indicate the range of free parameter values for which the model-data RMS error increases by less than 10%. The erosion coefficients at Ocean Beach (squares) have been multiplied by 10 to increase visibility. (d) Squared correlation R^2 between observed and modeled shoreline location (MHW at Ocean Beach, MSL at the southern California beaches). Parameter and R^2 values for sections with $R^2 < 0.6$ are shown in light gray.

parameter values. For example, accretion coefficients C^+ at Ocean Beach are usually only constrained within about an order of magnitude. Representative parameter values for each site are obtained by averaging over all (retained) sections (Table 1).

[21] The free parameters $C^{\pm}$ (1) and relative wave energy disequilibrium determine the shoreline change rate, and a (3) specifies the change in the equilibrium wave energy for a given change in shoreline location. These parameters relate wave properties to changes in shoreline location, and are therefore comparable between different sites. However, the free parameter b (3) relates the shoreline changes to the relative shoreline position S, which is defined independently at each site as fluctuations about the temporal mean shoreline position, and is therefore not comparable or transportable between sites.

[22] The time to adjustment (e-folding scale) to equilibrium $[aC^{\pm}E^{1/2}]^{-1}$ (5) is inversely proportional to H_s ($E = H_s^2/16$) and to $aC^{\pm}$. At Ocean Beach, $aC^{\pm}$ is smaller than at the other sites with finer sand (Table 1 and Figure 7), and thus has longer adjustment timescales. For a step change to a constant 1 m significant wave height H_s, the accretion e-folding timescale [C^+ in (5)] is approximately 2 months at Torrey Pines and 4 months at Ocean Beach (Table 1). For a typical large winter storm at Ocean Beach with H_s = 4 m, the erosion e-folding timescale decreases to approximately 1 week at Torrey Pines and 1 month at Ocean Beach.

[23] The longer response time at Ocean Beach characterizes the observed mediated response of shoreline location to highly energetic waves. Wave energy E is on average 8 times larger at Ocean Beach than at Torrey Pines, with comparably larger seasonal fluctuations (Figures 9g and 9h). However, the average vertical change near the shoreline location (calculated as the average vertical change of sand levels between the measured shoreline locations in subsequent surveys) at Ocean Beach is only about a factor of 2 larger than at Torrey Pines (typical values are 1.5 and 0.8 m, Figures 9c and 9d). The observed horizontal shoreline location displacements also differ by less than a factor of 2, with about 30 m of change for the Torrey Pines Beach MSL contour (e.g., Figure 9a, section T3) and about 45 m for the Ocean Beach MHW contour (e.g., Figure 9b, section OB8). Recall that MHW changes are about 20% less than MSL contour changes at OB. Even allowing for

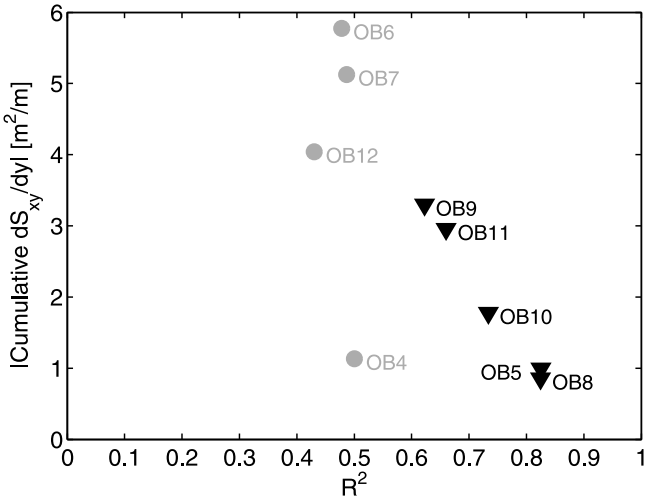

Figure 8. For each Ocean Beach alongshore section, the absolute value of the cumulative (for the duration of the survey period) alongshore radiation stress gradient dS_{xy}/dy on the 10 m depth contour versus R^2, the squared correlation coefficient between observed and modeled shoreline location. The cumulative dS_{xy}/dy, a proxy for the magnitude of time-integrated alongshore transport gradients (e.g., divergence of the drift), neglects contributions from other radiation stress terms. Gray circles and black triangles are locations with $R^2 < 0.6$ and $R^2 > 0.6$, respectively. At OB6, OB7, and OB12, R^2 is relatively low and the drift divergence proxy is relatively high, suggesting that neglected effects of alongshore transport degrade model performance.

this difference, Ocean Beach and Torrey Pines seasonal shoreline excursions differ by less than a factor of 2.

[24] The coarser sand grains at Ocean Beach (0.3 mm compared with 0.2 mm at Torrey Pines) may stabilize the Ocean Beach shoreline, requiring larger wave energy events to mobilize sand grains and causing slower transport rates, yielding smaller horizontal and vertical excursions than would occur with the same wavefield and finer sand [e.g., *Dean*, 1977; *Wright et al.*, 1985]. For example, a series of numerical simulations of beach profile changes suggest that increasing the median sand grain size from 0.2 mm to 0.3 mm decreases the change rates by a factor of 4 [*Kriebel and Dean*, 1993]. Time series of shoreline change and waves at many beaches are needed to establish empirically the dependence of model free parameters on grain size.

[25] A proxy (dS_{xy}/dy) for the alongshore gradients of alongshore transport (e.g., the divergence of the drift, neglected in the model) are on average much larger at Ocean Beach than Torrey Pines (Figures 9e and 9f). At Ocean Beach, locations with the largest proxy alongshore gradients are usually less well modeled (lower R^2, Figure 8), indicating the possible importance of alongshore transport gradients, and these locations are excluded from the site averages of the free parameters. Nevertheless, the effects of neglected alongshore sediment transport gradients, repeated beach nourishments in 10–14 m water depth, and changes in the San Fransisco Bar [*Dallas and Barnard*, 2009] on the estimated free parameter values (Table 1) are unknown. The model results are expected to be degraded at sites where alongshore processes have a significant role in controlling seasonal and multiyear shoreline change.

[26] The Ocean Beach observations are unique: seasonal shoreline change was monitored for several years along several kilometers of a high-energy beach with well-estimated wave conditions (Figure 4). The model free parameters were calibrated using the full time series of available observations, and previous tests at Torrey Pines Beach [*Yates et al.*, 2009] show that calibration using shorter observation periods or lacking a range of beach state and wave conditions may decrease the model skill. Given model coefficients and hypothetical wavefields, longer-term predictions of shoreline change may be made, but caution is necessary, as the model skill is unknown when applied to wave and shoreline scenarios well outside of the calibration values.

4.2. Alternative Model Formulations

[27] Using 6 years of shoreline position observations from the Gold Coast, Australia, *Davidson et al.* [2010] developed an equilibrium model

$$\frac{dS}{dt} = b + c\Omega^k(t)(\Omega_0 - \Omega(t)), \tag{6}$$

where c, k and Ω_0 are model free parameters, and b is a constant linear trend in shoreline location that is unrelated to the wavefield.

[28] Wave forcing and shoreline disequilibrium in (6) are characterized with Dean's parameter Ω, rather than wave energy E (1). At southern California sites, model performance is not substantially altered by replacing E in (1) with the cross-shore radiation stress, or by using a power other than 1/2 in $E^{1/2}$ [*Yates et al.*, 2009, Figure 8]. However, similar to the southern California sites, model skill at Ocean Beach decreases when E is replaced with Ω (Figure 10).

[29] *Davidson et al.* [2010] (6) uses a single response parameter c, whereas (1) allows different accretion and erosion responses (C^+ and C^-). Using C = constant ($C^+ = C^-$) in (1) causes less than a 10% reduction in average R^2 values

Table 1. Model Free Parameters for Each Survey Site[a]

Survey Site	a ($\times 10^{-3}$ m^2 m^{-1})	C^- (m h^{-1} m^{-3})	C^+ (m h^{-1} m^{-3})	Erosion Timescale (days)	Accretion Timescale (days)
Ocean Beach	−3.6 ± 2.3	−0.54 ± 0.47	−0.83 ± 0.63	43 ± 39	107 ± 66
Camp Pendleton	−8.5 ± 1.7	−1.15 ± 0.20	−1.24 ± 0.22	4 ± 1	16 ± 3
Cardiff	−4.2 ± 1.0	−0.96 ± 0.29	−1.52 ± 1.25	11 ± 3	40 ± 23
Torrey Pines	−4.5 ± 2.0	−1.38 ± 0.88	−1.16 ± 0.88	9 ± 4	52 ± 29

[a]For each survey site, mean (section averaged), and standard deviation (between sections) of model free parameters equilibrium slope a, erosion rate coefficient C^-, accretion rate coefficient C^+ (defined in (1)–(3)), and the erosion and accretion e-folding scales ($[aC^{\pm}E^{1/2}]^{-1}$) for significant wave heights of H_s = 4 m and H_s = 1 m ($E = H_s^2/16$), respectively.

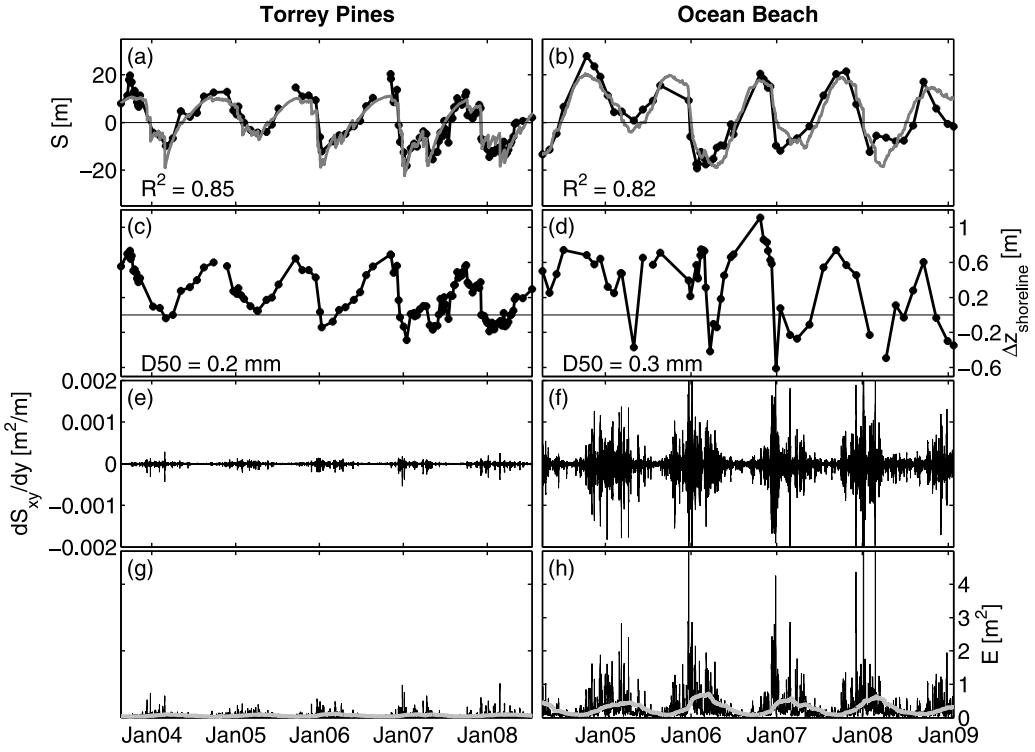

Figure 9. For Torrey Pines alongshore section TP3 (Figure 9, left) and Ocean Beach alongshore section OB8 (Figure 9, right): (a and b) S, observed (black) and equilibrium model (dark gray) shoreline location; (c and d) $\Delta z_{shoreline}$, average vertical change near the shoreline position; (e and f) dS_{xy}/dy, hourly radiation stress gradient; and (g and h) E, hourly wave energy (black) and 90 day average wave energy (gray).

at Ocean Beach and Torrey Pines (Figure 10). At least for these two data sets, a free model parameter in (1) can be eliminated with little degradation in model performance, even though different physical mechanisms are thought to control erosion and accretion.

[30] In (1)–(3), the equilibrium wave condition $E_{eq}(S)$ that determines the sign of the disequilibrium varies as a linear function of the beach state. Thus, moderate energy waves erode an accreted beach, but accrete an eroded beach. In contrast, Ω_0 in (6) is a constant, and a given wave condition always causes erosion, or always causes accretion (for a fixed grain size). With $E_{eq}(S)$ equal to a constant in (1), the model performance at both sites is strongly reduced relative to a linearly varying $E_{eq}(S)$ (Figure 10). With the free parameters C^+, C^-, and E_{eq} constants selected to maximize R^2 in each 500 m section, R^2 (averaged over all 500 m sections) decreases from 0.81 to 0.24 at Torrey Pines, and from 0.62 to 0.16 at Ocean Beach (Figure 10). At these sites, it is critical to include in $E_{eq}(S)$ a dependence on beach state S. However, (6) with constant Ω_0 yields relatively high R^2 at a Gold Coast site [*Davidson et al.*, 2010].

4.3. Transportability of Model Free Parameters

[31] The transportability between beaches of this (and similar) empirically derived models is understood poorly. The qualitative evaluation of the transportability of the model free parameters to San Onofre is an initial attempt to determine the dependence of free parameters on physical variables.

[32] San Onofre Beach in southern California has moderate wave energy, similar to Torrey Pines Beach, but coarser sand (0.3 mm), similar to Ocean Beach. Shoreline displacements at San Onofre are only a few meters (comparable to measurement errors), vary significantly between adjacent

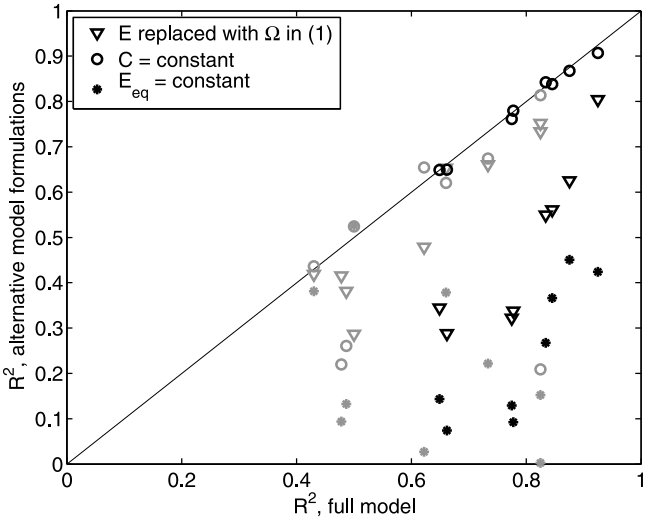

Figure 10. Correlation coefficients (R^2) obtained using the full model (1) and alternative model formulations (see legend) for each alongshore location at Ocean Beach (gray) and Torrey Pines Beach (black).

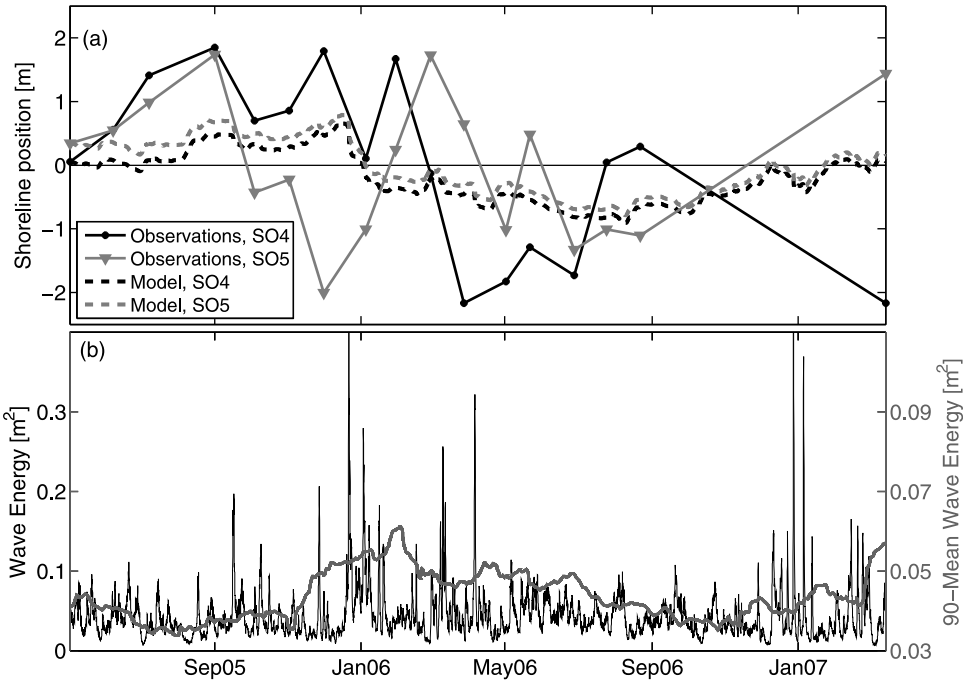

Figure 11. (a) Shoreline location (mean removed) at San Onofre sections SO4 and S05 versus time. Observations (solid lines) and equilibrium model results (dashed lines, estimated using site-averaged response coefficients from Ocean Beach) are significantly (95% confidence interval) correlated at S04 (R^2 = 0.32) but not at S05 (R^2 = 0.09). (b) Hourly (black line) and 90 day average (gray line) wave energy at San Onofre.

sections, and are not seasonal even though the wave energy varies seasonally (Figure 11). When the model coefficients are tuned to the observations, San Onofre shoreline changes were not well predicted (R^2 is low) by the equilibrium model. *Yates et al.* [2009] concluded that the model performed poorly because of the low signal-to-noise ratio at this relatively stable beach.

[33] To test the transportability of model coefficients between beaches with similar sand grain size, equilibrium model predictions were made at San Onofre using the average (neglecting sites discussed in section 3.2) Ocean Beach free parameters $C^{\pm}$ and a and the relative shoreline position b calculated with the San Onofre observations. Predicted seasonal shoreline changes are ±1 m and are qualitatively similar to the observed ±2 m (Figure 11). This consistency suggests response coefficients may be transportable between sites with similar grain size and different wave climates. Thus far the model has been tested only at sites with similar geomorphological properties (i.e., mesotidal beaches forming a single offshore bar in winter months), and optimal model free parameters may differ between beaches with similar grain size but contrasting geomorphological characteristics (associated, for example, with different sediment supplies). The effects of alongshore transport will in some cases also differentiate beaches with similar wave climates and sand grain size, further limiting the model transportability. Although there are many complicating factors, model transportability is supported by the success of simple parameterizations (for example measured with Ω [*Wright and Short*, 1984; *Wright et al.*, 1985]) suggesting that beaches with similar grain size and wave characteristics tend to form similar morphologic (i.e., dissipative, intermediate, and reflective) beach states.

4.4. Equilibrium and Average Wave Correlation Models

[34] The equilibrium model (1) relates changes in shoreline location dS/dt to the hourly wave energy E and the corresponding equilibrium wave energy E_{eq} (3). Whereas average wave correlation models often relate shoreline location S^{corr} to weekly to monthly averaged wave energy $\overline{E}$ or other wave properties

$$S^{corr}(t) = d_1\overline{E_N}(t-\tau) + d_2, \tag{7}$$

where $\overline{E}$ is here defined as the centered average wave energy over N days, τ is a time lag, and constants d_1 and d_2 define the linear regression slope and intercept. Squared correlations R^2 between the observed shoreline position S^{obs} (or an EOF proxy) and weekly to monthly averaged wave energy $\overline{E}$ are significant both at Ocean Beach [*Hansen and Barnard*, 2010] (Figure 3), and elsewhere [e.g., *Miller and Dean*, 2007]. At Ocean Beach, the maximum correlation is observed near a time lag $\tau = -60$ days and with N = 110 day wave averaging, and R^2 remains elevated (>0.7) over a broad range of values of τ and N near the maximum correlation. As expected for seasonally cyclic variables, R^2 between S^{obs} and $\overline{E}$ are elevated for ranges of lagged τ, separated by about 180 days (Figure 12a). The maximum S^{obs} (widest beach) consistently occurs at the end of summer in September or October, about 60 days after the minimum average wave energy $\overline{E}$ in July or August (vertical dashed

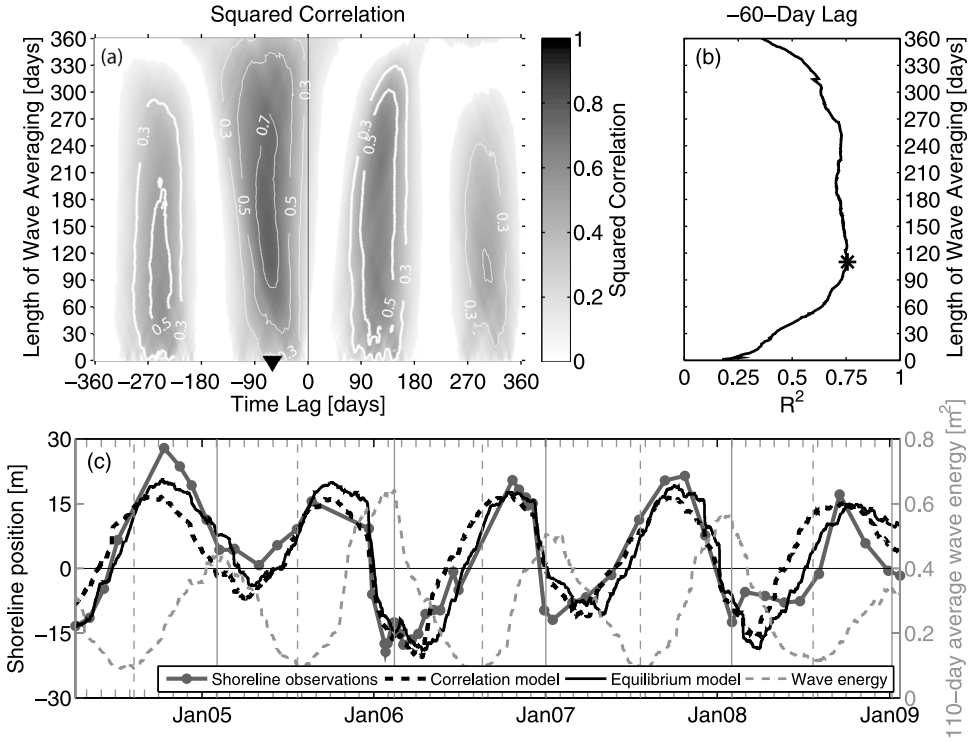

Figure 12. Correlation between time-averaged wave energy $\overline{E}$ and shoreline position S at Ocean Beach alongshore section OB8: (a) Contours of squared correlation R^2 (gray scale at right) versus time lag τ and duration of wave averaging N. Thin and thick lines are negative and positive correlations, respectively, and the black triangle indicates the cross section shown in Figure 12b. (b) R^2 for a −60 day time lag versus duration of wave energy averaging N. The asterisk indicates the maximum correlation at a −60 day time lag, at approximately $N = 110$ day wave averaging. (c) Observed S^{obs}, equilibrium model S^{eq}, and average wave correlation model S^{corr} ($\tau = -60$, $N = 110$) shoreline location versus time. The 110 day averaged wave energy $\overline{E}$ is also shown, with annual maxima and minima indicated by the dashed and solid gray vertical lines, respectively. Correlations are S^{obs} and S^{corr}, $R^2 = 0.76$; S^{obs} and S^{eq}, $R^2 = 0.82$.

grey line in Figure 12c). The minimum S^{obs} (narrowest beach) occurs between January and March, with a less clearly defined lag relative to the maximum $\overline{E}$, which usually occurs in January. For relatively short wave-averaging periods ($N < 2$ days), S^{obs} and $\overline{E}$ are only weakly correlated ($R^2 < 0.3$) because wave conditions can vary much faster than the beach morphology adjusts (e.g., during storms [e.g., *Morton et al.*, 1995]). For seasonal wave-averaging periods (of a few months), R^2 correlations between S^{obs} and $\overline{E}$ are elevated because both the shoreline location and storms are seasonal. Equilibrium model predictions, the result of integrating (1) over time, reproduce the observed high R^2 between S^{obs} and $\overline{E}$ averaged over a few months, and S^{eq}, S^{obs}, and S^{corr} (with 60 day lag and 110 day averaging) are mutually correlated (Figure 12c).

5. Summary

[35] Four years of shoreline elevation surveys at Ocean Beach, San Francisco, California were used to extend the validation and calibration of an existing equilibrium shoreline change model to a higher-energy beach with coarser sand grains. Wave energy and shoreline location, defined as the cross-shore location of the MHW elevation contour, vary seasonally. The equilibrium shoreline change model (1) relates the rate of horizontal shoreline displacement to the hourly wave energy E and wave energy disequilibrium ΔE (the difference between E and the equilibrium wave energy E_{eq} that would cause no change in the present shoreline location). On this beach with relatively energetic winter storms and summer lulls, an equilibrium model responding to rapid (hourly) changes in wave energy predicts the observed, strong seasonal shoreline variations that are also highly correlated with the time-lagged, weekly to seasonally averaged wave energy. The equilibrium shoreline change model previously showed skill in reproducing more than 5 years of shoreline observations from Torrey Pines Beach, CA, a site with significantly less (factor of 8) energetic winter waves but only a moderately smaller (factor of 2) seasonal cycle in shoreline location.

[36] At Ocean Beach, the model simulates the effects of cross-shore transport on shoreline location, and the effects of strong tidal and wave-driven alongshore currents are neglected. The highest correlations are observed at locations lacking significant temporal trends, which are hypothesized to be caused by these neglected alongshore processes. Values for the model free parameters at Ocean Beach, averaged over alongshore locations where the equilibrium model has good skill, are used to characterize the shoreline response to energetic waves on a beach with medium-grained sand. The

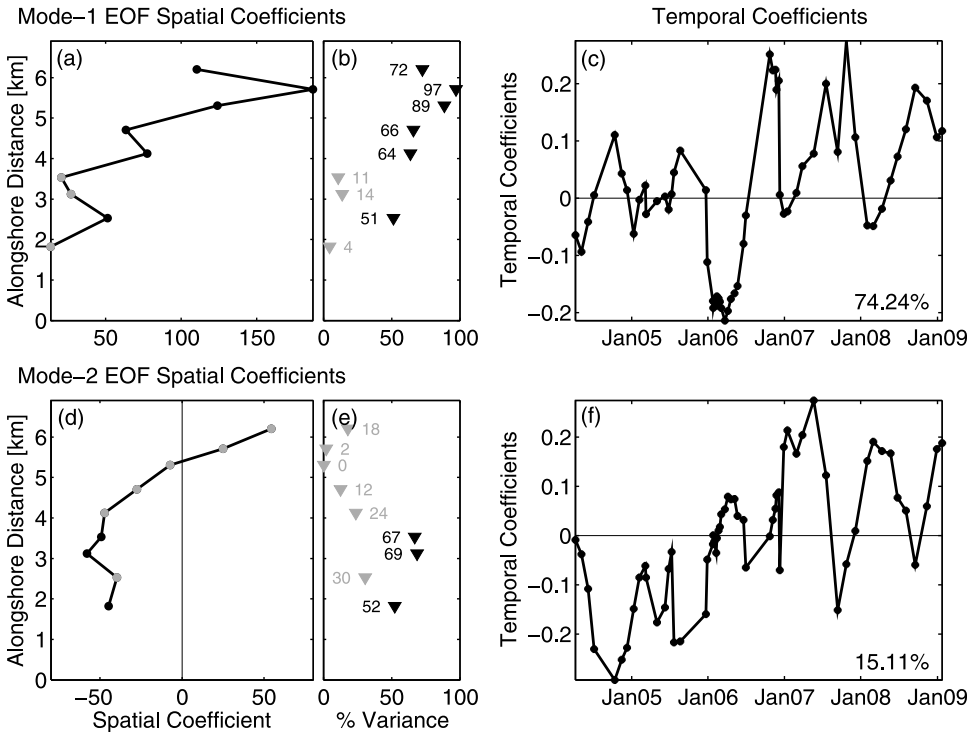

Figure A1. Mode 1 (Figure A1, top) and mode 2 (Figure A1, bottom) EOFs of shoreline location: (a and d) spatial coefficients, (b and e) percentage of variance explained by each mode for each alongshore section, and (c and f) temporal coefficients and percentage of total shoreline variance explained by each mode for all alongshore locations. Alongshore locations where less than 50% of the variance is explained by each EOF mode are in gray.

reduced mobility of the coarser sand (0.3 mm median diameter) at Ocean Beach is reflected in lower model erosion rate coefficients at Ocean Beach than at Torrey Pines Beach (0.2 mm median diameter). Model shoreline response coefficients at Ocean Beach are qualitatively consistent with the observed stability of a similar grain size beach (San Onofre, in southern California) that is exposed to much lower (factor of 8) energy winter waves. The consistency suggests that the response coefficients depend on grain size and may be transportable between sites with similar grain size and different wave climates. Additional observations over a wide range of wave conditions and beach morphologies are needed to establish if simple, equilibrium "rules" can be used to model shoreline change on beaches dominated by cross-shore transport.

Appendix A

[37] EOFs of shoreline location at OB4–OB12 (the nine alongshore locations with adequate data) show that the mode 1 EOF of seasonal shoreline change represents 74% of the total shoreline variance (Figures A1a–A1c). However, less than 15% of the shoreline variance at OB4, OB6, and OB7 is explained in the mode 1 EOF, whereas more than 50% of the shoreline variance is explained at the other locations (Figure A1b).

[38] The mode 2 EOF represents only 15% of the total variance, but more than 50% of the variance at OB4, OB6, and OB7 (Figures A1d–A1f). The mode 2 temporal coefficients show both seasonal variability and a long-term trend (Figure A1f), with a shift from long-term erosion to accretion near alongshore location OB10 (Figure A1d), in agreement with *Hansen and Barnard* [2010]. Even with a linear trend removed from each alongshore location, time series of shoreline location at OB4, OB6, and OB7 remain different from other regions.

[39] Possible reasons for the anomalous behavior include the attachment of the San Francisco Bar to the shoreline and an oblique nearshore bar near OB7 (section 2) that causes wave refraction and alongshore variability in wave heights and alongshore currents. Strong tidal currents are also present due to the proximity of the Golden Gate, and alongshore currents are spatially variable and can exceed 1 m/s near the surf zone [*Barnard et al.*, 2007]. To reduce scour around the Southwest Ocean Outfall in 10–14 m depth (not shown), 230,000 m^3 of sediment from the Main Ship Channel was placed in 9–14 m water depth, offshore of the erosion "hot spot" near OB4 (Figure 2b), in May 2005, 2006, and 2007. Although clear subaerial beach accretion was not observed in response to the nourishments [*Barnard et al.*, 2009], changes in nearshore sediment availability could contribute to alongshore variability in shoreline response.

[40] **Acknowledgments.** Bathymetric and topographic data collection was supported by the USGS and the San Francisco District of the United States Army Corps of Engineers. Wave data collection was supported by the United States Army Corps of Engineers and the California Department of Boating and Waterways. The Coastal Data Information Program, managed by Julie Thomas, maintained and operated the wave network.

References

Aubrey, D. G., D. L. Inman, and C. D. Winant (1980), The statistical prediction of beach changes in southern California, *J. Geophys. Res.*, *85*, 3264–3276.

Barnard, P. L., J. Eshleman, L. Erikson, and D. M. Hanes (2007), Coastal processes study at Ocean Beach, San Francisco, CA: Summary of data collection 2004-1006, *Open File Rep. 2007-1217*, U.S. Geol. Surv., Reston, Va.

Barnard, P. L., L. H. Erikson, and J. E. Hansen (2009), Monitoring and modeling shoreline response due to shoreface nourishment on a high-energy coast, *J. Coastal Res.*, *56*, 29–33.

Bruun, P. (1954), Coastal erosion and development of beach profiles, *Tech. Memo. 44*, U.S. Army Corps of Eng., Washington, D. C.

Dallas, K. L., and P. L. Barnard (2009), Linking human impacts within an estuary to ebb-tidal delta evolution, *J. Coastal Res.*, *56*, 713–716.

Davidson, M. A., and I. L. Turner (2009), A behavioral template beach profile model for predicting seasonal to interannual shoreline evolution, *J. Geophys. Res.*, *114*, F01020, doi:10.1029/2007JF000888.

Davidson, M. A., R. P. Lewis, and I. L. Turner (2010), Forecasting seasonal to multi-year shoreline change, *Coastal Eng.*, *57*, 620–629, doi:10.1016/j.coastaleng.2010.02.001.

Dean, R. G. (1977), Equilibrium beach profiles: U.S. Atlantic and Gulf coasts, *Ocean Eng. Rep. 12*, Dep. of Civ. Eng., Univ. of Del., Newark, Del.

Dean, R. G. (1991), Equilibrium beach profiles: Characteristics and applications, *J. Coastal Res.*, *7*, 53–84.

Dubois, R. N. (1990), Barrier-beach erosion and rising sea level, *Geology*, *18*, 1150–1152.

Eshleman, J. E., P. L. Barnard, E. L. H., and D. M. Hanes (2007), Coupling alongshore variations in wave energy to beach morphologic change using the SWAN wave model at Ocean Beach, San Francisco, CA, paper presented at 10th International Workshop on Wave Hindcasting and Forecasting, Oahu, Hawaii, Environ. Can., 11–16 Nov.

Hansen, J. E., and P. L. Barnard (2010), Sub-weekly to interannual variability of a high-energy shoreline, *Coastal Eng.*, *57*, 959–972, doi:10.1016/j.coastaleng.2010.05.011.

Haxel, J. H., and R. A. Holman (2004), The sediment response of a dissipative beach to variations in wave climate, *Mar. Geol.*, *206*, 73–99.

Kriebel, D. L., and R. G. Dean (1993), Convolution method for time-dependent beach profile response, *J. Waterway Port Coastal Ocean Eng.*, *119*, 204–226.

Larson, M., and N. C. Kraus (1989), SBEACH: Numerical model for simulating storm-induced beach change, *Tech. Rep. CERC-89-9*, U.S. Army Corps of Eng., Vicksburg, Miss.

Larson, M., M. Capobianco, and H. Hanson (2000), Relationship between beach profiles and waves at Duck, North Carolina, determined by canonical correlation analysis, *Mar. Geol.*, *160*, 275–288.

Lee, G., R. J. Nicholls, and W. A. Birkemeier (1998), Storm-driven variability of the beach-nearshore profile at Duck, North Carolina, USA, 1981–1991, *Mar. Geol.*, *148*, 163–177.

List, J. H., and A. S. Farris (1999), Large-scale shoreline response to storms and fair weather, in *Coastal Sediments '99*, edited by N. C. Kraus and W. G. McDougal, pp. 1324–1338, Am. Soc. of Civ. Eng., Reston, Va.

List, J. H., A. S. Farris, and C. Sullivan (2006), Reversing storm hotspots on sandy beaches: Spatial and temporal characteristics, *Mar. Geol.*, *226*, 261–279.

Miller, J. K., and R. G. Dean (2004), A simple new shoreline change model, *Coastal Eng.*, *51*, 531–556.

Miller, J. K., and R. G. Dean (2006), An engineering scale model for predicting the shoreline response to variations in waves and water levels, paper presented at 7th International Conference on HydroScience and Engineering, Am. Soc. of Civ. Eng., Philadelphia, Pa., 10–13 Sep.

Miller, J. K., and R. G. Dean (2007), Shoreline variability via empirical orthogonal function analysis: Part II. Relationship to nearshore conditions, *Coastal Eng.*, *54*, 133–150.

Morton, R. A., J. C. Gibeaut, and J. G. Paine (1995), Meso-scale transfer of sand during and after storms: Implications for prediction of shoreline movement, *Mar. Geol.*, *126*, 161–179.

National Oceanic and Atmostpheric Administration (2010), Tides and Currents, http://tidesandcurrents.noaa.gov/, Cent. of Oper. Prod. and Serv., Silver Spring, Md.

O'Reilly, W. C., and R. T. Guza (1998), Assimilating coastal wave observations in regional swell predictions. Part I: Inverse methods, *J. Phys. Oceanogr.*, *28*, 679–691.

Quartel, S., A. Kroon, and B. G. Ruessink (2008), Seasonal accretion and erosion patterns on a microtidal sandy beach, *Mar. Geol.*, *250*, 19–33, doi:10.1016/j.margeo.2007.11.003.

Wentworth, C. K. (1922), A scale of grade and class terms for clastic sediments, *J. Geol.*, *30*, 377–392.

Wright, L. D., and A. D. Short (1984), Morphodynamic variability of surf zones and beaches: A synthesis, *Mar. Geol.*, *56*, 93–118.

Wright, L. D., A. D. Short, and M. O. Green (1985), Short-term changes in the morphodynamic states of beaches and surf zones: An empirical predictive model, *Mar. Geol.*, *62*, 339–364.

Yates, M. L., R. T. Guza, and W. C. O'Reilly (2009), Equilibrium shoreline response: Observations and modeling, *J. Geophys. Res.*, *114*, C09014, doi:10.1029/2009JC005359.

P. L. Barnard and J. E. Hansen, Pacific Science Center, United States Geological Survey, 400 Natural Bridges Dr., Santa Cruz, CA 95060, USA.

R. T. Guza and W. C. O'Reilly, Scripps Institution of Oceanography, University of California, San Diego, 9500 Gilman Dr., La Jolla, CA 92093-0209, USA.

M. L. Yates (corresponding author), Bureau de Recherches Géologiques et Minières, 3 Ave. Claude Guillemin, F-45060 Orléans, France. (myates@coast.ucsd.edu)